

Microstructure evolution and mechanical properties of ZK60 magnesium alloy produced by SSTM and RAP route in semi-solid state

Chang-peng WANG¹, Ying-ying ZHANG², Di-fan LI¹, Hua-sheng MEI¹, Wei ZHANG¹, Jie LIU¹

1. No.59 Institute of China Ordnance Industry, Chongqing 400039, China;

2. Chang'an Automobile Stock Co., Ltd, Chongqing 401120, China

Received 4 January 2013; accepted 15 March 2013

Abstract: The microstructure evolution and mechanical properties of a ZK60 magnesium alloy produced by the semi-solid thermal transformation (SSTM) route and the recrystallization and partial melting (RAP) route were studied, respectively. The microstructure evolution during partial remelting was studied at different temperatures for different time. The tensile mechanical properties of thixoformed components by the two routes at room temperature were examined. The results show that coalescence is dominant in the SSTM alloy and Ostwald ripening is dominant in the RAP alloy. Compared with the SSTM route, the RAP route can produce finer semi-solid microstructure under the similar isothermal holding condition. The microstructure of the RAP alloy is much more spheroidized compared with the SSTM alloy. Thixoforming for the ZK60 magnesium alloy produced by the SSTM and RAP route results in successful filling of the die, and the thixoforming process improves the mechanical properties of ZK60 magnesium alloy. The RAP alloy shows significantly advantageous mechanical properties over that of the SSTM alloy.

Key words: ZK60 magnesium alloy; semi-solid thermal transformation (SSTM); recrystallization and partial melting (RAP) route; microstructure evolution; mechanical properties

1 Introduction

Magnesium alloys have received much attention as important materials in aerospace, automobile and electronic industries due to their low density, high specific strength and stiffness, good electromagnetic shielding characteristics and good machinability [1,2]. Currently, almost magnesium alloys are used mainly in high pressure die-casting (HPDC) form for structural components in the automobile industry. However, HPDC components contain a substantial amount of porosity due to gas entrapment during die filling which affects the mechanical properties adversely [3]. It has been recognized that semi-solid processing offers significant advantages over traditional casting routes [4–6]. Thixoforming is a semi-solid processing route which involves the preparation of a feedstock material with thixotropic characteristics, reheating the solid feedstock material and shaping the semi-solid billet to components, so the main requirement of this process is that the microstructure of the starting material must be spheroidal

rather than dendritic [7,8]. There are several routes to obtain the spheroidal microstructure, such as strain-induced melt activation (SIMA), recrystallization and partial remelting (RAP) and semi-solid thermal transformation (SSTM) [9,10]. The SIMA route involves working above the recrystallization temperature followed by reheating to the semi-solid state. The advantages of the SIMA route are that some alloys can supply in the extruded state in any case and the spheroids are more fully rounded. The RAP route involves working below the recrystallization temperature followed reheating to the semi-solid state. On the semi-solid state, recrystallization occurs and liquid penetrates the recrystallized boundaries resulting in spheroids which were surrounded by liquid. A significant difference between the RAP route and the SIMA route is that the former involves warm working below the recrystallization temperature, while the latter involves hot working above recrystallization temperature. The SSTM route involves simply heating a dendritic structure to the semi-solid temperature range for a period of time sufficient to get a spheroidal structure.

Up to now, the evolution of microstructure produced by the SIMA route in magnesium alloys was reported that the SIMA route can obtain fine microstructures [11,12], but there is only a few information concentrating on the RAP route [13] and the SSTM route [14]. The SSTM route is a promising alternative for the production of feedstocks for thixoforming due to its simplicity. Moreover, magnesium alloys currently used in semi-solid processing are restricted to a few commercial alloys such as AZ91D [15,16] and AZ31 [17–19]. There are few reports concerning the microstructure evolution and thixoforging of ZK60 magnesium alloys produced by the RAP and SSTM route. In the present study, the microstructure evolution of ZK60 magnesium alloy produced by the SSTM and RAP route is examined in the semi-solid state and compared under the almost similar conditions. Moreover, the mechanical properties of the thixoformed SSTM alloy and the thixoformed RAP alloy are also presented.

2 Experimental

Alloy ingots of ZK60 were produced from high purity Mg (99.9%), Zn (99.9%) and Mg–30Zr (mass fraction, %) master alloys in an electric resistance furnace under the mixed atmosphere of CO₂ and SF₆ with the volume ratio of 100:1. When the temperature reached 780 °C, molten metal was stirred homogeneously for about 8 min and held for 20 min, after that the metal was poured in a metal mold with a diameter of 140 mm. ZK60 alloy with a composition of Mg–4.5Zn–0.5Zr in mass fraction. As-cast ingots were machined into cylinder-shaped ingots with dimensions of d120 mm× 120 mm. The cylinder-shaped ingot was then subjected to deformation by compression at 360 °C, and the compression ratio was 50%. The compression ratio was defined as the relative reduction of height of the sample, which was $(H_0 - H)/H_0$, where H_0 is the original height and H is the height after compression. This was designated by the deformed samples.

Investigation of microstructure evolution during partial remelting was done on as-cast and deformed samples with a diameter of 8 mm and a length of 12 mm. The isothermal holding experiments were performed in a vertical tube furnace under the protective atmosphere of flowing argon. Samples were partially remelted isothermally at various temperatures and time in the range of 5–60 min. To preserve the morphology and content of the unmelted fraction, in removal from the furnace, the samples should be immediately quenched in cold water after removing from the furnace. Care was taken to ensure that the beginning time of isothermal holding was defined as the time when the samples were

heated to predefined temperature without holding partially remelted. The samples were sectioned at a sufficient depth from the surface to avoid errors in the microstructural analysis due to anomalous coarsening of grains on the surface. Mean grain size and shape factor of solid particles were calculated from the following equations: $D = (4A/\pi)^{1/2}$ and $F = (4\pi A)/P^2$, where A and P are area and perimeter of grains respectively [20,21]. For each sample, measurements were taken from the whole sectioned area with 250–300 grains per sample. The approximate relationship between solid fraction f_s and temperature (T) was determined using the Scheil equation: $f_s = 1 - [(T_M - T_L)/(T_M - T)]^{1/(1-k_0)}$, where T_M is the melting point of pure metal, T is the temperature of isothermal holding, T_L is the liquidus temperature of alloy and k_0 is the equilibrium distribution coefficient [22]. In this study, T_M , T_L and k_0 were taken as 650, 629 °C and 0.123, respectively. Therefore, the expected solid fraction (f_s) of ZK60 alloy was 0.78 at 570 °C in this study.

For the thixoforming, the cylindrical slugs with a diameter of 58 mm and a length of 40 mm were machined from as-cast and deformed ZK60 bars, respectively. Thixoforming was carried out on the vertically upwards acting thixoforming press. The as-cast slugs and deformed ZK60 slugs were heated to 570 °C for 10 min isothermal holding. The temperature of the slug was monitored by a K-type thermocouple embedded in the slug. After reaching the required temperature, the thermocouple was removed and the heated slug was placed into the die. The preheat temperature of the die was 350 °C. Molybdenum disulphide (MoS₂) was used as a lubricant. During thixoforming, the punch speed was about 1 mm/s. The pressure exerted by the punch on the slug was gradually increased to a pre-determined level of 200 MPa and kept at this level for 60 s.

Microstructure was examined by optical microscopy (OM). Samples for tensile testing were machined from the side wall of thixoformed components and were tested using an Instron 5569 material testing machine at a cross head speed of 1 mm/min. Tensile curves were analyzed to assess the ultimate tensile strength (UTS), yield strength (YS) and elongation to failure. Each tensile value was the average of at least five measurements.

3 Results

3.1 As-cast and deformed microstructures

Figure 1 shows the optical micrographs of as-cast and deformed ZK60 magnesium alloy. As shown in Fig. 1(a), the grains were coarse and equiaxed (100–150 μm), some low-melting point phase (as the second phase) was precipitated as discontinuous network primarily at grain boundaries. The formation of the second phase was

attributed to the non-equilibrium solidification. As shown in Fig. 2(b), the grains underwent severe plastic deformation and the boundaries of the grains were not clear, the brittle second phase was elongated and distributed over the grain boundaries and showed a remarkable orientation along the deformation direction.

3.2 Microstructure evolution of SSTM and RAP processed ZK60 alloys during partial remelting with increasing holding time

The as-cast ingot during partial remelting can be classified as being consistent with the SSTM route due to the fact that it is unrecrystallized microstructure. Figure 2 shows the microstructure evolution of SSTM processed ZK60 alloy during partial remelting at 570 °C ($f_s=0.78$) for different isothermal holding time. According to Fig. 2, 5 min isothermal holding at 570 °C was not enough for spheroidization. Solid grains were still stick together and

the separation did not occur. This can be attributed to low liquid fraction, so the solid grains were not completely penetrated by liquid film (Fig. 2(a)). Increasing isothermal holding time to 10 min resulted in the increased liquid fraction and the separation of contacted solid grains, and some individual solid grains were subjected to spheroidization (Fig. 2(b)). When the isothermal holding time was up to 20 min, parts of the corners and edges of polygonal solid grains melted, which resulted in the spheroidization of polygonal solid grains and the increase in the amount of liquid phase, the solid grains were almost perfectly spheroidal, but the microstructure was heterogeneous (Fig. 2(c)). Simultaneously, liquid was gathered in pools and some small solid grains suspended in liquid pools. A comparison between Figs. 2(b) and (c) showed that significant grain coarsening occurred in the semi-solid state after 20 min. Disappearance of grain boundaries

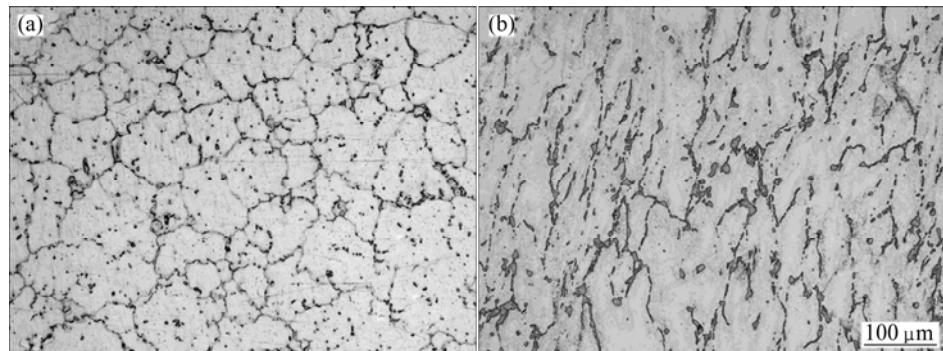


Fig. 1 Optical images of as-cast (a) and deformed (b) ZK60 magnesium alloys

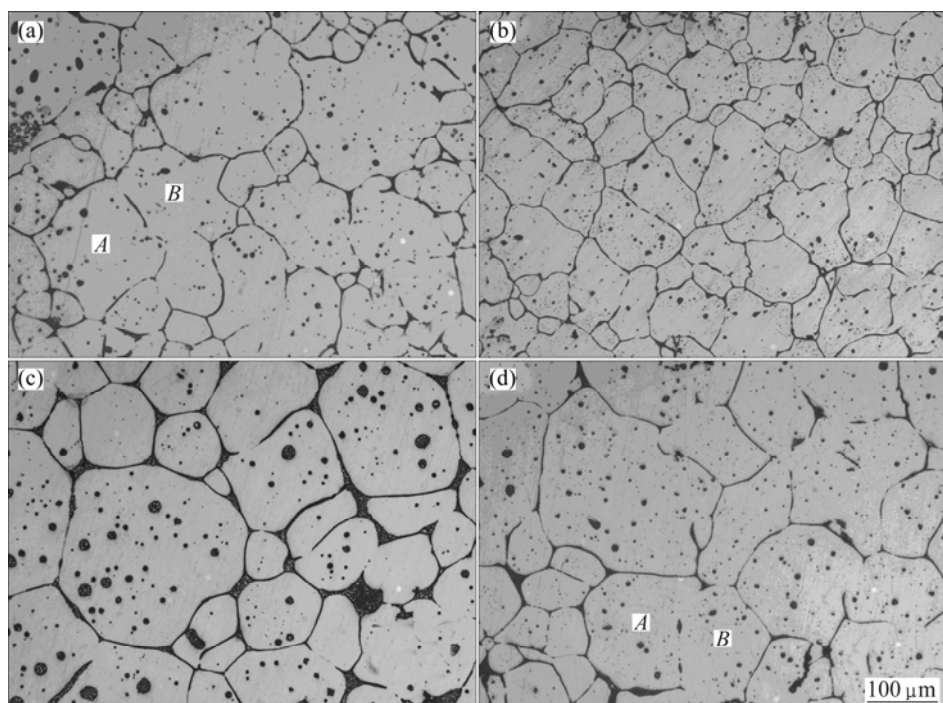


Fig. 2 Microstructure evolution of SSTM processed ZK60 alloy during partial remelting at 570 °C ($f_s=0.78$) for 5 min (a), 10 min (b), 20 min (c) and 60 min (d)

resulted in coalescence as shown in Fig. 2(c), where the grain boundaries between grains *A* and *B* disappeared, and led to the formation of a larger grain with irregular shape. With further prolonging holding time, the growing tendency of the solid grains was obvious and grain coarsening by coalescence resulted in the irregular shape grains (Fig. 2(d)).

The deformed ingot during partial remelting can be classified as being consistent with the RAP route. Figure 3 shows the microstructure evolution of SSTM processed ZK60 alloy during partial remelting at 570 °C ($f_s=0.78$) for different isothermal holding time. Following partial remelting state, the microstructure mainly consisted of spheroidal recrystallized grains with some internally entrapped liquid. When the holding time stayed for 5 min,

recrystallization occurred entirely. Conglomerated structures were separated into individual solid grains because of liquid penetration. The microstructure in the semi-solid state consisted of fine and almost perfectly globular recrystallized grains which had intragranular liquid droplets; solid grains surrounded by liquid had undergone a significant degree of spheroidization, as shown in Fig. 3(a). With prolonging holding time, the thickness of liquid film around the solid grains was thicker, but the grain size had no obvious change (Figs. 3(b) and (c)). However, there was a significant grain coarsening occurring in the semi-solid state when the isothermal holding time was up to 60 min, as shown in Fig. 3(d).

Figure 4 shows the variation of grain size and shape

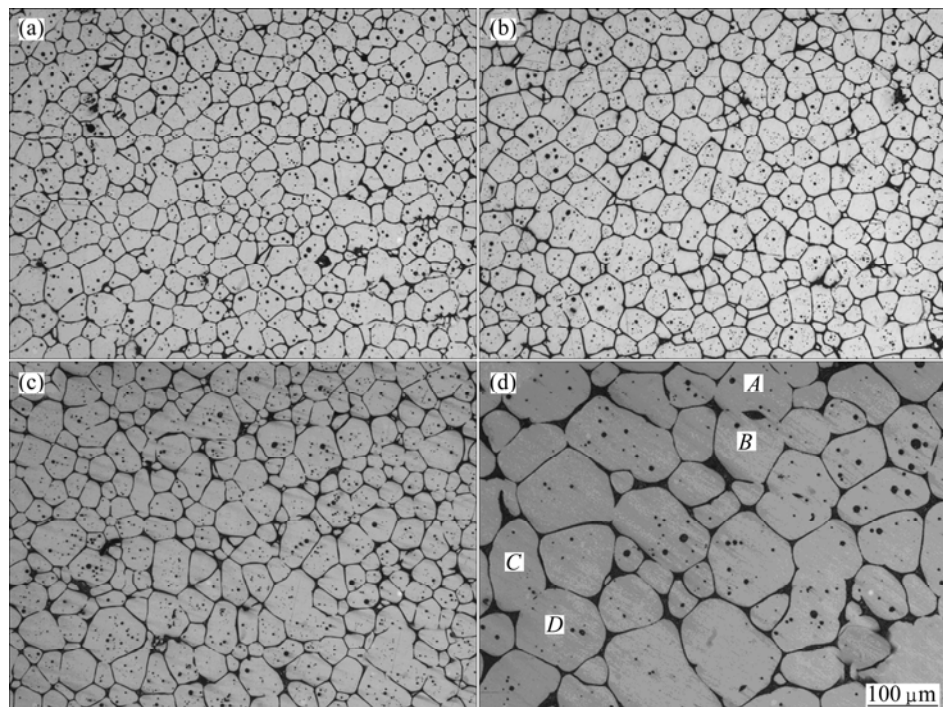


Fig. 3 Microstructure evolution of RAP processed ZK60 alloy during partial remelting at 570 °C ($f_s=0.78$) for 5 min (a), 10 min (b), 20 min (c) and 60 min (d)

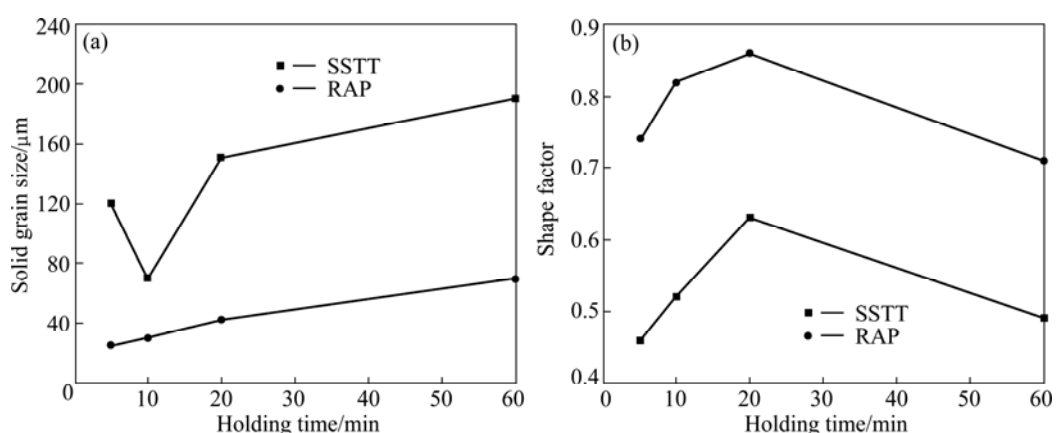


Fig. 4 Grain size (a) and shape factor (b) for SSTM and RAP processed alloys during partial remelting at 570 °C ($f_s=0.78$) for different holding time

factor for the SSTM processed alloy and the RAP processed alloy during partial remelting at 570 °C ($f_s=0.78$) for different isothermal holding time. It was shown that the solid grain size decreased initially and then increased with the isothermal holding time increasing for the RAP processed alloy. However, for the SSTM processed alloy, the grain size measurement showed a continuous increase of the grain size with prolonging holding time, as shown in Fig. 4(a). Compared with the SSTM processed alloy, the RAP processed alloy has finer solid particles under the similar isothermal holding conditions. As shown in Fig. 4(b), the variations of shape factor in both the SSTM processed alloy and the RAP processed alloy exhibited a similar trend that the solid grains became increasingly spheroidal after isothermal holding for 5 min. However, the spheroids developed more angular shapes and the shape factor decreased slightly after 40 min isothermal holding. Moreover, it also can be seen from Fig. 4(b) that the degree of spheroidization in the RAP processed alloy was also better than that in the SSTM processed alloy.

3.3 Tensile mechanical properties

Figure 5 shows the photographs of two successfully thixoformed demonstrator components. The parts of starting materials are ZK60 magnesium alloys produced

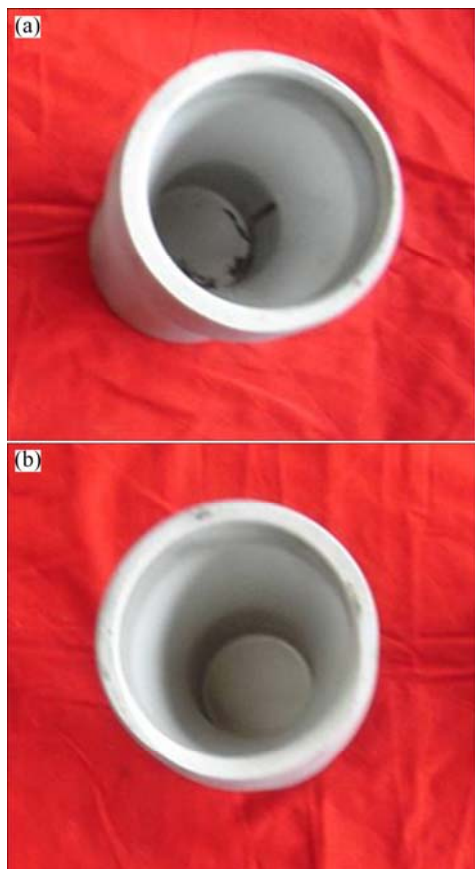


Fig. 5 Photography of two successfully thixoformed components produced by SSTM (a) and RAP (b) routes

by SSTM and RAP route. The reproduction of the barrel-shaped parts was good, and no problem was experienced in filling the thin-walled sections. Figure 6 shows the tensile mechanical properties of as-cast and thixoformed ZK60 alloys produced by the SSTM and RAP routes. For the deformed alloy, there was strong dependence of mechanical properties on the methods of semi-solid processing. The results show that the ultimate tensile strength (UTS), yield strength (YS) and elongation of thixoformed ZK60 alloy produced by the SSTM route were 214 MPa, 146 MPa and 4%, respectively. The UTS, YS and elongation of thixoformed ZK60 alloy produced by the RAP route were 302 MPa, 210 MPa and 12%, respectively. Compared with those of thixoformed ZK60 alloy produced by the SSTM route, the UTS, YS and elongation of thixoformed ZK60 alloy produced by the RAP route were further improved. Moreover, the tensile mechanical properties of the thixoformed ZK60 alloys were better than the as-cast ZK60 alloys. The UTS, YS and elongation of as-cast ZK60 alloys were 187 MPa, 135 MPa and 3.5%, respectively.

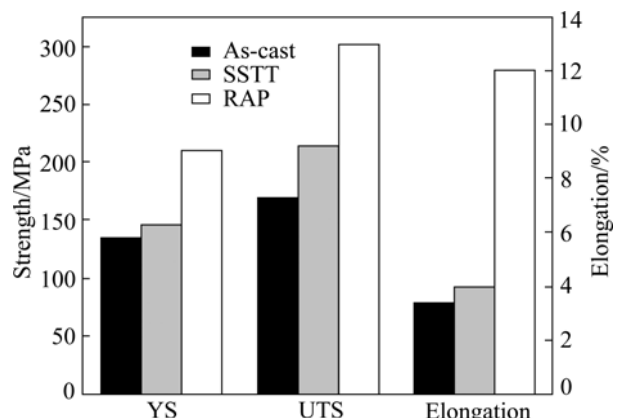


Fig. 6 Tensile mechanical properties of as-cast ZK60 alloys and thixoformed ZK60 alloys produced by SSTM route and RAP route

4 Discussion

4.1 Microstructural evolution during partial remelting

It is well established that the system reduces energy by the elimination of the interfaces of high curvature and two mechanisms are generally considered to control solid grain coarsening: coalescence and Ostwald ripening [23–25]. Coalescence is usually defined as the formation of one large particle upon contact of two smaller ones, and coalescence by grain boundary migration is dominant at short time after liquid is formed and at low volume fractions of liquid. Ostwald ripening is dominant at a longer time and at high volume fractions of liquid. Ostwald ripening involves the growth of large particles

at the expense of small particles, and is governed by the Gibbs-Thompson effect which alters the chemical potential of solutes at the particle–liquid interface, depending on the curvature of the interface. Compared with the grain size exhibited by the processed RAP alloy, the SSTM processed alloy obtained much more serious coarse grains. In the SSTM processed alloy, the thickness of liquid film which was around the solid grains was thicker with prolonging holding time in the initial of isothermal holding time, because the solid–solid interfacial energy was higher than the solid–liquid interfacial energy, and the liquid phase would penetrate into the solid grains in order to reduce the interfacial energy [26]. Such as the liquid film between grains A and B in Fig. 2(a), with the growing of the liquid phase, grains A and B were separated completely in the end, which made the number of the grains increase and the grain size decrease, as shown in Fig. 2(b). With prolonging isothermal holding time, individual grains coarsened because these individual grains had relatively coarse size and irregular shape; liquid phase was few and nonuniform, under this circumstance coalescence playing a significant role in grain coarsening which caused grains continuously to grow [27]. However, due to the diffusion of liquid phase, the corners and edges of solid grains melted in order to reduce the solid–liquid interfacial energy, so the shape factor of grains was also increased. Therefore, solid grains gradually become more spheroidal [28]. When the isothermal holding time was up to 60 min, coarsening in the alloy was controlled by solid–solid contacts and grain contacts led to an increase in grain growth rates and especially the irregular shape, namely, the grains A and B merged into a larger and longer grain which was irregular shown in Fig. 2(d), so the shape factor of grains was slightly decreased.

In the RAP processed alloy, because underwent plastic severe deformation, the overall grain boundary and subgrain boundary area may increase [29]. On one hand, this led to the greater potential for the development of recrystallization nuclei. On the other hand, this resulted in an increase in the amount of stored energy in the alloy and increased driving force towards recrystallization [30]. Because enough strain hardening was introduced into the alloy, complete recrystallization and fragmentation were achieved in a short time, so the grain was fine when the isothermal holding time was just 5 min. It can be seen from Fig. 3 that the grain size has no obvious increase when the isothermal holding time was controlled in 20 min, because the globular grains were almost free of entrapped pools which were homogeneously surrounded by liquid films. Under this circumstance, the contribution of coalescence to the coarsening has been suppressed, and grain coarsening in

the RAP processed alloy was mainly controlled by diffusion through liquid rather than by the solid–solid contacts. So, the Ostwald ripening was thought to play a dominant role and the corners and edges of solid grains were melted which led to the shape factor of grains increase. When the isothermal holding time was up to 60 min, coalescence played the dominant role, microstructure exhibited significant grain coarsening and the shape factor decreased. As shown in Fig. 3(d), two spheroidal grains (such as grains A and B or grains C and D) which were similar in size merged into larger and irregular-shaped grains.

From Figs. 2 and 3 we can know that the microstructure of the RAP processed alloy is finer and much more is spheroidized compared with the SSTM processed alloy under the similar isothermal holding condition. We can also find that properly prolonging holding time is favorable for liquid penetration of solid grain boundaries and for the improvement of degree of spheroidization, but too long holding time results in excessive grain coarsening. Therefore, the isothermal holding time may be controlled in 40 min both for the SSTM processed alloy and the RAP processed alloy.

4.2 Tensile mechanical properties

The tensile mechanical properties of the thixoformed ZK60 alloys were better than as-cast ZK60 alloys. Moreover, the thixoformed ZK60 alloys produced by the RAP route were better than those produced by the SSTM route. The superior mechanical properties of the components thixoformed by the RAP route had two reasons. First, thixoformed components inherited the mechanical properties from their original feedstocks, the mechanical properties of thixoformed components depended on the properties of original feedstocks, and mechanical properties were largely determined by the number of defects present in the sample. For the alloy produced by the RAP route, some casting deficiencies, such as gas pores, hot cracks and microstructural non-uniformity have been eliminated or reduced during compression with 50% compressive rate [31–33]. Second, the RAP route produced ideal, fine and homogeneous semi-solid microstructures, in which completely spheroidal primary solid grains were entrapped with a little number of liquid droplets, such microstructures are ideal for thixoforming [34]. Moreover, the RAP route obtained more finer recrystallized solid grains during partial remelting, and small-grained alloy would have a higher density of grain boundaries per unit volume which could effectively hinder the dislocation motion. So, it was reasonable for the RAP processed alloy to exhibit excellent mechanical properties.

5 Conclusions

1) With prolonging holding time, the RAP route produces finer semi-solid microstructure compared with the SSTM processed alloy under the similar isothermal holding condition. In the SSTM processed alloy, coalescence mechanism plays a dominant role. In the RAP processed alloy, the Ostwald ripening is thought to be the dominant grain coarsening mechanism and that coalescence is also present, although exerting a minor role.

2) Both for the SSTM processed alloy and the RAP processed alloy, the isothermal holding time may be controlled in 40 min.

3) Thixoforming for ZK60 magnesium alloy is produced by the SSTM route and the RAP processed route results in successful filling of the die. Thixoforming process improves the mechanical properties of ZK60 magnesium alloy. Compared with the SSTM processed alloy, the RAP processed alloy shows significant advantageous mechanical properties over that of the SSTM processed alloy.

References

- [1] CHEN Qiang, LIN Jun, SHU Da-yu, HU Chuan-kai, ZHAO Zu-de, KANG Feng, HUANG Shu-hai, YUAN Bao-guo. Microstructure development, mechanical properties and formability of Mg–Zn–Y–Zr magnesium alloy [J]. Materials Science and Engineering A, 2012, 554: 129–141.
- [2] JI Z S, HU M L, SUGIYAMA S M, YANAGIMOTO J. Formation process of AZ31B semi-solid microstructures through strain-induced melt activation method [J]. Materials Characterization, 2008, 59(7): 905–911.
- [3] CHEN Qiang, SHU Da-yu, HU Chuan-kai, ZHAO Zu-de, YUAN Bao-guo. Grain refinement in an as-cast AZ61 magnesium alloy processed by multi-axial forging under the multitemperature processing procedure [J]. Materials Science and Engineering A, 2012, 541: 98–104.
- [4] YI M, SUMIO S, JUN Y. Microstructural evolution during RAP process and deformation behavior of semi-solid SKD61 tool steel [J]. Journal of Materials Processing Technology, 2012, 212(8): 1731–1741.
- [5] LUO Shou-jing, CHEN Qiang, ZHAO Zu-de. Effects of processing parameters on the microstructure of ECAE-formed AZ91D magnesium alloy in the semi-solid state [J]. Journal of Alloys and Compounds, 2009, 477: 602–607.
- [6] ZHANG Liang, WU Guo-hua, WANG Shao-hua, DING Wen-jiang. Effect of cooling condition on microstructure of semi-solid AZ91 slurry produced via ultrasonic vibration process [J]. Transactions of Nonferrous Metals Society of China, 2012, 22(10): 2357–2363.
- [7] ZHAO Zu-de, CHENG Yuang-sheng, CHEN Qiang, WANG Yan-bin, SHU Da-yu. Reheating and thixoforging of ZK60+RE alloy deformed by ECAE [J]. Transactions of Nonferrous Metals Society of China, 2010, 20: 178–182.
- [8] JIANG Ju-fu, WANG Ying, QU Jian-jun, DU Zhi-ming, LUO Shou-jing. Numerical simulation and experiment validation of thixoforming angle frame of AZ61 magnesium alloy [J]. Transactions of Nonferrous Metals Society of China, 2010, 20(3): 888–892.
- [9] CHEN Qiang, YUAN Bao-guo, ZHAO Gao-zhan, SHU Da-yu, HU Chuan-kai, ZHAO Zu-de, ZHAO Zhi-xiang. Microstructural evolution during reheating and tensile mechanical properties of thixoforged AZ91D-RE magnesium alloy prepared by squeeze casting–solid extrusion [J]. Materials Science and Engineering A, 2012, 537: 25–38.
- [10] ZHAO Zu-de, CHEN Qiang, KANG Feng, SHU Da-yu. Microstructural evolution and tensile mechanical properties of thixoformed AZ91D magnesium alloy with the addition of yttrium [J]. Journal of Alloys and Compounds, 2009, 482: 455–467.
- [11] XU Hong-yu, JI Ze-sheng, HU Mao-liang, WANG Zhen-yu. Microstructure of AZ91D magnesium alloy semi-solid billets prepared by SIMA method from chips [J]. Transactions of Nonferrous Metals Society of China, 2010, 20(S3): s749–s753.
- [12] ZHAO Zu-de, CHEN Qiang, TANG Ze-jun, HU Chuan-kai. Microstructural evolution and tensile mechanical properties of AM60B magnesium alloy prepared by the SIMA route [J]. Journal of Alloys and Compounds, 2010, 497: 402–411.
- [13] ZHAO Zu-de, CHEN Qiang, CHAO Hong-ying, HUANG Shu-hai. Microstructural evolution and tensile mechanical properties of thixoforged ZK60-Y magnesium alloys produced by two different routes [J]. Materials and Design, 2010, 31: 1906–1916.
- [14] CHENG Yuan-sheng, CHEN Qiang, HUANG Zhe-qun, HUANG Shu-hai. Microstructure evolution and thixoextrusion of AZ91D magnesium alloy produced by SSTM [J]. Transactions of Nonferrous Metals Society of China, 2010, 20(S3): s739–s743.
- [15] YANG Liu-qing, KANG Yong-lin, ZHANG Fan, XU Jun. Microstructure and mechanical properties of rheo-diecasting AZ91D Mg alloy [J]. Transactions of Nonferrous Metals Society of China, 2010, 20(S3): s862–s867.
- [16] CHEN Qiang, LUO Shou-jing, ZHAO Zu-de. Microstructural evolution of previously deformed AZ91D magnesium alloy during partial remelting [J]. Journal of Alloys and Compounds, 2009, 477: 726–731.
- [17] WU She-yan, JI Ze-sheng, RONG Shou-fan, HU Mao-liang. Microstructure and mechanical properties of AZ31B magnesium alloy prepared by solid-state recycling process from chips [J]. Transactions of Nonferrous Metals Society of China, 2010, 20(5): 783–788.
- [18] ZHAO Hu, HE Liang-ju, LI Pei-jie. Microstructure of asymmetric twin-roll cast AZ31 magnesium alloy [J]. Transactions of Nonferrous Metals Society of China, 2011, 21(11): 2372–2377.
- [19] HUANG Guang-sheng, LI Hong-cheng, SONG Bo, ZHANG Lei. Tensile properties and microstructure of AZ31B magnesium alloy sheet processed by repeated unidirectional bending [J]. Transactions of Nonferrous Metals Society of China, 2010, 20(1): 28–33.
- [20] ZHAO Zu-de, CHEN Qiang, HUANG Shu-hai, KANG Feng, WANG Yan-bin. Microstructure and tensile properties of AM50A magnesium alloy prepared by recrystallisation and partial melting process [J]. Transactions of Nonferrous Metals Society of China, 2010, 20(9): 1630–1637.
- [21] YANG Ming-bo, PAN Fu-sheng, CHENG Ren-ju, SHEN Jia. Effects of holding temperature and time on semi-solid isothermal heat-treated microstructure of ZA84 magnesium alloy [J]. Transactions of Nonferrous Metals Society of China, 2008, 18(3): 566–572.
- [22] CHEN Qiang, ZHAO Zu-de, ZHAO Zhi-xiang, HU Chuan-kai, SHU Da-yu. Microstructure development and thixoextrusion of magnesium alloy prepared by repetitive upsetting-extrusion [J]. Journal of Alloys and Compounds, 2011, 509: 7303–7315.
- [23] ZHAO Zu-de, CHEN Qiang, HU Chuan-kai, HUANG Shu-hai, WANG Yuan-qing. Near-liquidus forging, partial remelting and

thixoforging of an AZ91D+Y magnesium alloy [J]. Journal of Alloys and Compounds, 2009, 485: 627–636.

[24] LI Jing-yuan, XIE Jian-xin, JIN Jun-bing, WANG Zhi-xiang. Microstructural evolution of AZ91 magnesium alloy during extrusion and heat treatment [J]. Transactions of Nonferrous Metals Society of China, 2012, 22(5): 1028–1034.

[25] ZHAO Zu-de, CHEN Qiang, WANG Yan-bin, SHU Da-yu. Effect of predeformation on semi-solid microstructure of ZK60+RE magnesium alloy [J]. Transactions of Nonferrous Metals Society of China, 2009, 19(3): 535–539.

[26] ZHAO Zu-de, CHEN Qiang, WANG Yan-bin, SHU Da-yu. Microstructural evolution of an ECAE-formed ZK60-RE magnesium alloy in the semi-solid state [J]. Materials Science and Engineering A, 2009, 506: 8–15.

[27] ZHAO Zu-de, CHEN Qiang, HU Chuan-kai, SHU Da-yu. Microstructure and mechanical properties of SPD-processed an as-cast AZ91D+Y magnesium alloy by equal channel angular extrusion and multi-axial forging [J]. Materials and Design, 2009, 30: 4557–4561.

[28] CHEN Qiang, SHU Da-yu, ZHAO Zu-de, ZHAO Zhi-xiang, WANG Yan-bin, YUAN Bao-guo. Microstructure development and tensile mechanical properties of Mg–Zn–RE–Zr magnesium alloy [J]. Materials and Design, 2012, 40: 488–496.

[29] YING Tao, HUANG Jian-ping, ZHENG Ming-yi, WU Kun. Influence of secondary extrusion on microstructures and mechanical properties of ZK60 magnesium alloy [J]. Transactions of Nonferrous Metals Society of China, 2012, 22(5): 1896–1901.

[30] CHEN Qiang, ZHAO Zhi-xiang, SHU Da-yu, ZHAO Zu-de. Microstructure and mechanical properties of AZ91D magnesium alloy prepared by compound extrusion [J]. Materials Science and Engineering A, 2011, 528: 3930–3934.

[31] YAN Hong, WANG Jian-jin. Thixotropic compression deformation behavior of SiCp/AZ61 magnesium matrix composites [J]. Transactions of Nonferrous Metals Society of China, 2010, 20(S3): s811–s814.

[32] ZHAO Zu-de, CHEN Qiang, CHAO Hong-ying, HU Chuan-kai, HUANG Shu-hai. Influence of equal channel angular extrusion processing parameters on the microstructure and mechanical properties of Mg–Al–Y–Zn alloy [J]. Materials and Design, 2011, 32: 575–583.

[33] HUANG Hai-jun, CHEN Ti-jun, MA Ying, HAO Yuan. Microstructural evolution during solution treatment of thixoformed AM60B Mg alloy [J]. Transactions of Nonferrous Metals Society of China, 2011, 21(4): 745–753.

[34] QIU Wei, HAN En-hou, LIU Lu. Effect of heat treatment on microstructures and mechanical properties of extruded-rolled AZ31 Mg alloys [J]. Transactions of Nonferrous Metals Society of China, 2010, 20(S3): s481–s487.

SSTT 和 RAP 方法得到的 ZK60 镁合金的组织变化和力学性能

王长朋¹, 张营营², 李迪凡¹, 梅华生¹, 张 帷¹, 刘 杰¹

1. 中国兵器工业 第五九研究所, 重庆 400039;

2. 重庆长安汽车股份有限公司, 重庆 401120

摘要: 研究了分别由半固态热成形方法(SSTT)和部分重熔再结晶方法(RAP)得到的 ZK60 镁合金在一定温度下显微组织随等温时间的变化和触变成形试样的力学性能。结果表明, 合并长大机制在 SSTT 合金的组织变化中占主导地位, 熟化机制在 RAP 合金的组织变化中起主要作用。在相同的等温条件下, 与 SSTT 方法相比, RAP 方法可以得到更细小的半固态显微组织, RAP 合金组织比 SSTT 合金组织更圆整。由 SSTT 方法和 RAP 方法得到的 ZK60 镁合金触变成形后均得到了较理想的成形件, 触变成形工艺提高了材料的力学性能。与 SSTT 合金相比, RAP 合金具有更优越的力学性能。

关键词: ZK60 镁合金; 半固态热成形; 部分重熔再结晶; 组织变化; 力学性能

(Edited by Xiang-qun LI)